Available online at www.sciencedirect.com
SCIENCE DIRECT
Journal of Molecular Catalysis A: Chemical 246 (2006) 206–211
JOURNAL OF MOLECULAR CATALYSIS A: CHEMICAL
www.elsevier.com/locate/molcata

Photocatalytic activity of dispersed TiO_2 particles deposited on glass fibers

Huogen Yu [a,b], S.C. Lee [a,*], Jiaguo Yu [b,*], C.H. Ao [a]

[a] *Department of Civil and Structural Engineering, Research Center for Environmental Technology and Management, The Hong Kong Polytechnic University, Hung Horn, Kowloon, PR China*
[b] *State Key Laboratory of Advanced Technology for Material Synthesis and Processing, Wuhan University of Technology, Wuhan 430070, PR China*

Received 28 September 2005; received in revised form 29 September 2005; accepted 7 November 2005
Available online 9 December 2005

Abstract

Anatase TiO_2 particles were uniformly and dispersedly deposited on the surface of glass fibers by a liquid phase deposition (LPD) method from a TiF_4 aqueous solution upon addition of H_3BO_3 at 60 °C and then calcined at 60, 300 and 500 °C. The photocatalytic activity of the samples was evaluated by the photocatalytic oxidation of nitrogen monoxide (NO) in the gaseous phase. It was found that calcination temperatures obviously influenced the surface morphology and photocatalytic activity of the TiO_2 particles deposited on the glass fibers. At 300 °C, the TiO_2 samples exhibited the highest photocatalytic activity for the photocatalytic oxidation of NO and for the further conversion of NO_2 (from NO_2 to HNO_3) due to the enhancement of crystallization of anatase TiO_2 particles. At 500 °C, the photocatalytic activity of the sample decreased significantly due to the dropping of many TiO_2 particles from the glass fibers. Compared with the TiO_2 film photocatalyst, the TiO_2 particles deposited on the glass fibers exhibited a lower deactivation rate.

Keywords: TiO_2 particles; Photocatalytic activity; Glass fibers; LPD; Deactivation rate; Nitrogen monoxide

1. Introduction

There is an increasing concern about the indoor air quality (IAQ) because the quality of indoor air has a direct impact on human healthy due to the lengthened inhabitation in the indoor environment [1–3]. Modern buildings have been designed to be more airtight in order to decrease the consumption of energy since energy conservation measures were instituted in office buildings in the 1970s due to energy crisis. However, the decrease of the intake of fresh air resulted in the build-up of various indoor air pollutants. Indoor domestic appliances, such as gas stoves and heaters, could be the main sources of pollutants due to the burning of coal, oil and natural gas, particularly in the areas that are poorly ventilated [4]. Moreover, a great number of materials used in construction, furnishing and insulation further increased the amount of pollutants [5]. Among various pollutants, nitrogen oxides are the most common pollutants found in the indoor environment [3]. It is well known that the lengthened exposure to the nitrogen oxides with a high concentration can cause headache, fatigue, dizziness, difficult breaking, throat spasms and fluid build-up in the lungs. Studies have indicated that NO concentration is usually in the range 70–500 ppb in the indoor environment [6,7]. Owing to its low concentration, it is not suitable and effective to use traditional remediation technique such as adsorption and filtration to reduce or eliminate the pollutants [8,9]. Moreover, the use of adsorbents merely transfers pollutants from the gaseous phase to the solid phase and easily causes post-disposal and regeneration problems. Despite the importance of IAQ, only few studies have reported on the feasibility of applying photocatalytic technology for the removal of indoor air pollutants [2,3].

Photocatalysis technique provides a very promising solution for the removal of indoor air pollutants and TiO_2 is one of the most effective photocatalysts due to its strong oxidizing power, non-toxicity and long-term photostability [10–20]. When TiO_2 powder is used as a photocatalyst for water purification, it shows high photocatalytic activity due to its large surface area. However, conventional powdered photocatalysts have a serious limitation—the need for post-treatment separation in a slurry system after photocatalytic reaction. Meanwhile, mobile photocatalyst powder is also not applicable for air purifi-

* Corresponding authors.
E-mail addresses: ceslee@polyu.edu.hk (S.C. Lee), jiaguoyu@yahoo.com (J. Yu).

1381-1169/$ – see front matter © 2005 Elsevier B.V. All rights reserved.
doi:10.1016/j.molcata.2005.11.007

cation, as it may contribute to respirable particles that cause adverse human health problems. Though this can be overcome by immobilizing TiO_2 particles as thin films on solid substrates [21–25], the formation of TiO_2 films on the substrates significantly reduced the specific surface area of TiO_2 photocatalysts, resulting in a decrease of photocatalytic activity. If anatase TiO_2 particles can be uniformly and dispersedly deposited on the surface of fibers, the prepared TiO_2 photocatalysts not only have a large surface area and keep high photocatalytic activity, but also can avoid the disadvantages of TiO_2 powdered photocatalysts. Therefore, it is very interesting to investigate the photocatalytic activity of the TiO_2 particles deposited on the fibers.

In the present work, anatase TiO_2 particles were uniformly and dispersedly deposited on the surface of the glass fibers from a TiF_4 aqueous solution upon addition of H_3BO_3 at 60 °C and then calcined at 60, 300 and 500 °C. The as-prepared TiO_2 samples were characterized with X-ray diffraction (XRD) and scanning electron microscopy (SEM). The photocatalytic activity of the samples was evaluated by the photocatalytic oxidation of nitrogen monoxide (NO) in the gaseous phase.

2. Experimental

2.1. Preparation

TiF_4 and H_3BO_3 were dissolved in distillated water in order to prepare the respective precursor solutions. The as-prepared aqueous solutions of TiF_4 and H_3BO_3 were mixed, stirred and used as a deposition solution. The initial concentrations of the deposition solution were 0.025 M TiF_4 and 0.075 M H_3BO_3. The pH value of the deposition solution was adjusted to ca. 2.0 using hydrochloric acid (1 M HCl) or aqueous ammonia (1 M NH_4OH). Then the glass fiber clothes ($0.1\,H \times 20.0\,L \times 20.0\,W$ cm) were immersed and suspended in a 250 ml deposition solution at 60 °C for 12 h. After the TiO_2-coated glass fibers were taken out and rinsed with distilled water, the samples were dried at 60 °C for 2 h and then calcined at 300 and 500 °C in air for 2 h, respectively. Apart from the above-described TiO_2 particle samples, TiO_2 film deposited on the stainless steel was also prepared under the same experimental conditions.

2.2. Characterization

X-ray diffraction (XRD) patterns were obtained on a Philips MPD 18801 X-ray diffractometer using Cu Kα irradiation at a scan rate of $0.05^\circ\ 2\theta\ S^{-1}$ and were used to determine the crystalline phase and the crystallite size. The accelerating voltage and the applied current are 35 kV and 20 mA, respectively. The scanning electron micrographs (SEM) were obtained on a Leica Stereoscan 440 microscope.

2.3. Photocatalytic activity

The evaluation of photocatalytic activity of the TiO_2 particle photocatalyst was performed in the gas phase by measuring the photocatalytic oxidation of NO, which was fed into a laboratory-scale continuous flow photoreactor. The inlet concentration of NO was 200 ppb. The detailed experimental set-up and process have been reported elsewhere [26]. A reactor with a volume of 18.6 L ($20.1\,H \times 44.2\,L \times 21\,W$ cm) and its surface coated with a teflon film (BYTAC Type AF-21) was used for this study. A 6 W 365 nm UV lamp (Cole-Parmer Instrument Co., USA) was used as light source and its intensity was determined with a UV meter (Spectroline DRC-100X). The UV lamp was horizontally placed at the upper part of the reactor, 14 cm from both ends. The UV intensity measured in all experiments was 600 μW/cm^2. The TiO_2 sample was supported by a teflon film and fixed horizontally at a vertical distance of 5 cm away from the UV lamp. Stainless steel sampling ports and teflon tubing were used to connect the reactor and the analytical instruments. A zero air generator (Thermo Environmental Inc., Model 111) was used to supply the air stream. The desired humidity of the flow was controlled by passing a zero air stream through a humidification chamber. The reactant stream and the zero air streams were pre-mixed in a gas blender (Advanced Pollution Instrumentation Inc., Model 700) and a mass flow controller controlled the desired flow. After the inlet and the outlet concentration of the target pollutants achieved equilibrium (30 min), the UV lamp was turned on and initiated the reaction. The concentration of NO was continuously measured by a Chemiluminescence NO analyzer (Thermo Environmental Instruments Inc., Model 42c), which monitored NO, NO_2 and NO_x (NO_x represents $NO + NO_2$) with a sampling rate of 0.7 L/min. The photocatalytic activity of TiO_2 particle photocatalyst was characterized by the removal rates of NO, NO_2 and NO_x. The NO, NO_2 and NO_x removal rates (%) are calculated according to the following equations [2,3]:

$$\text{NO removal}\,(\%) = \frac{[\text{NO}]_{\text{inlet}} - [\text{NO}]_{\text{outlet}}}{[\text{NO}]_{\text{inlet}}} \times 100\% \quad (1)$$

$$\text{NO}_2\ \text{removal}\,(\%) = \frac{[\text{NO}_2]_{\text{inlet}} - [\text{NO}_2]_{\text{outlet}}}{[\text{NO}]_{\text{inlet}}} \times 100\% \quad (2)$$

$$\text{NO}_x\ \text{removal}\,(\%) = \frac{[\text{NO}_x]_{\text{inlet}} - [\text{NO}_x]_{\text{outlet}}}{[\text{NO}]_{\text{inlet}}} \times 100\% \quad (3)$$

where $[NO]_{inlet}$, $[NO_2]_{inlet}$ and $[NO_x]_{inlet}$ represent the inlet pollutant concentrations and $[NO]_{outlet}$, $[NO_2]_{outlet}$ and $[NO_x]_{outlet}$ are the outlet concentrations measured at an irradiation time of 120 min after the UV lamp was turned on.

3. Results and discussion

3.1. Surface morphologies and crystalline phase

The glass fibers used as the substrates show a wide diameter distribution range from 100 nm to 2 μm. When the glass fibers were immersed into the deposition solution, TiO_2 particles were gradually deposited on their surface. The formation process of the TiO_2 particles on the glass fibers was reported in our previous study [26]. When the TiO_2-coated glass fibers were heat-treated at 300 °C, the morphology of the TiO_2 particles on the glass fibers has no obvious change. Fig. 1(a) and (b)

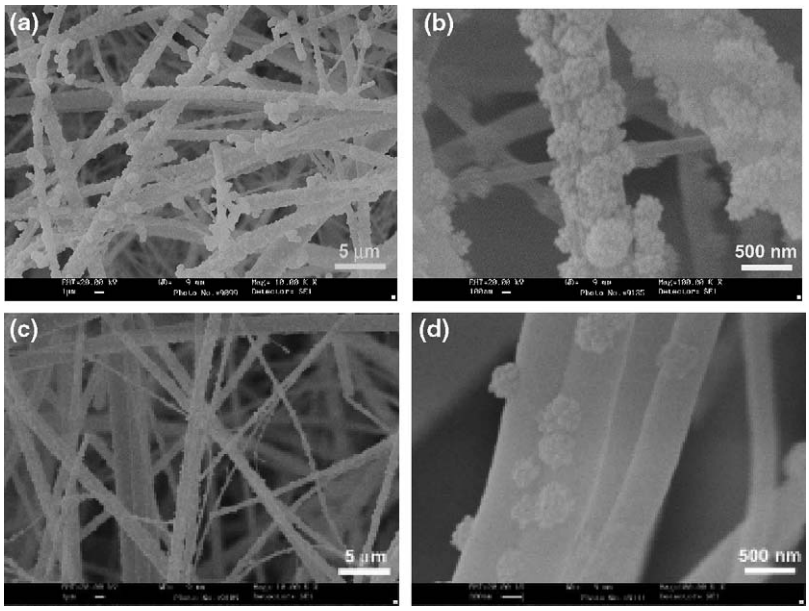

Fig. 1. SEM photographs of the TiO_2 particles deposited on the glass fibers and calcined at 300 °C ((a) and (b)) and 500 °C ((c) and (d)).

show the SEM images of the surface of the TiO_2-coated glass fibers calcined at 300 °C. It can be found that the TiO_2 particles with sizes of 200–400 nm are uniformly and dispersedly deposited on the surface of the glass fibers. Further, observation indicates that the TiO_2 particles deposited on the glass fibers are composed of many smaller TiO_2 particles with a size of 20–70 nm (as shown in Fig. 1(b)). At 500 °C, the number of the TiO_2 particles deposited on the glass fibers decrease significantly (as shown in Fig. 1(c) and (d)). This may be attributed to the difference in thermal expansion coefficients between TiO_2 and glass fibers, which causes the interfacial stresses and results in the dropping of TiO_2 particles from the surface of the glass fibers.

The intensities of X-ray diffraction peaks of the TiO_2 particle photocatalysts deposited on the glass fibers were very weak for phase analysis due to the limited amount of TiO_2 particles. To determine the crystalline phase and crystallite size of the TiO_2 particles deposited on the glass fibers, TiO_2 powders were also prepared from the same deposition solution without the addition of the glass fibers. Fig. 2 shows the XRD patterns of the TiO_2 powder samples calcined at 60, 300 and 500 °C. At 60 °C, only the diffraction peaks of anatase are observed. This indicates that crystalline anatase TiO_2 particles could be prepared at 60 °C. The average crystallite size of the TiO_2 powders was calculated according to Scherrer's equation from the (1 0 1) diffraction peak of anatase and was ca. 6 nm at 60 °C. With increasing calcination temperatures, the peak intensities of anatase increase and the width of the (1 0 1) peak becomes narrow, which is ascribed to the growth of anatase crystallites and the enhancement of crystallization. The average crystallite sizes of the TiO_2 powders calcined at 300 and 500 °C are ca. 10 and 15 nm, respectively. Therefore, it can be concluded that the TiO_2 particles deposited on the surface of the glass fibers (as shown in Fig. 1) consist of many smaller anatase TiO_2 crystallites.

3.2. Effect of calcination temperature on the photocatalytic activity

Fig. 3 shows the photocatalytic activity of the as-prepared TiO_2 particles deposited on the glass fibers at 60 °C for the photocatalytic oxidation of 200 ppb NO. It can be seen that prior to UV illumination, the adsorption and desorption of NO have reached an equilibrium. When UV lamp was turned on, the photocatalytic oxidation of NO was initiated immediately. The concentration of NO dropped rapidly in the first 20 min and then reached a lowest value of ca. 63 ppb. After that, the concentration of NO increased slightly with increasing irradiation time. This was ascribed to the accumulation of HNO_3 on the surface of TiO_2 particles, resulting in the deactivation of TiO_2 photocatalyst [27]. After UV irradiation for 120 min, the concentration of NO gradually reached a photo-steady-state concentration (ca.

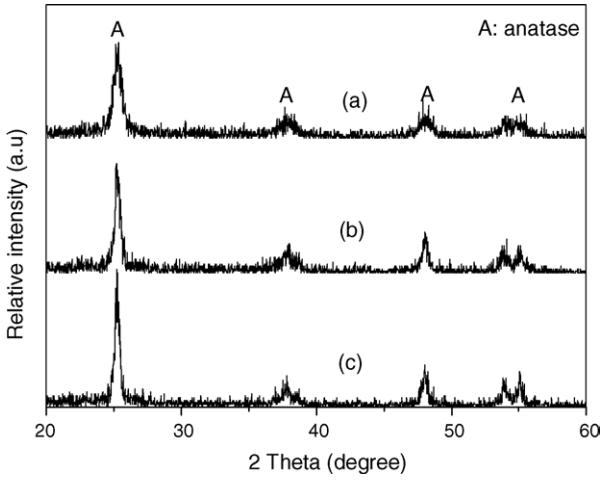

Fig. 2. XRD patterns of the TiO_2 powders calcined at 60 °C (a), 300 °C (b) and 500 °C (c).

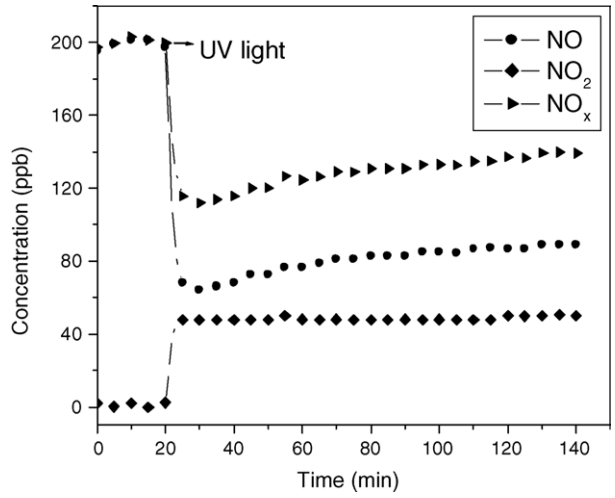

Fig. 3. Photocatalytic activity of the as-prepared TiO_2 particles deposited on the glass fibers at 60 °C for the photocatalytic oxidation of 200 ppb NO. Residence time: 11.4 min; humidity levels: 2100 ppmv.

88 ppb). However, the concentration of the generated NO_2 by the photocatalytic oxidation of NO almost kept a constant.

To evaluate the effect of calcination temperatures on the photocatalytic activity of TiO_2 particles deposited on the glass fibers, the prepared samples were then calcined at 300 and 500 °C for 2 h, respectively. When calcination temperature was higher than 500 °C, the fiber was easily destroyed due to its low melting point. Therefore, the maximum calcination temperature was limited to 500 °C. Table 1 lists the photocatalytic activities of the TiO_2 particles deposited on the glass fibers and calcined at 60, 300 and 500 °C. It can be observed that the removal rate of NO increases with increasing calcination temperatures. At 300 °C, the TiO_2 particle sample shows the highest photocatalytic activity. This is ascribed to the enhancement of crystallization of anatase TiO_2 particles (see Fig. 2). At 500 °C, the removal rate of NO obviously decreases from 64.87% (at 300 °C) to 19.35%. This is due to the dropping of a large number of TiO_2 particles from the surface of the glass fibers (as shown in Fig. 1(c) and (d)).

For the photocatalytic oxidation of NO, the following reactions may exist [28,29].

$$NO + HO_2^{\bullet} \rightarrow NO_2 + OH^{\bullet} \quad (4)$$

$$NO_2 + OH^{\bullet} \rightarrow HNO_3 \quad (5)$$

It is well known that nitrogen oxides (NO and NO_2) are a major pollution source in our environment and harmful to human health. Therefore, it is not enough to evaluate the photocatalytic activity of TiO_2 samples only by the removal rate of NO. More attention should be paid to the further conversion of NO_2 (from NO_2 to HNO_3), because HNO_3 is more easily removed in practice. During the photocatalytic oxidation of NO, NO_2 is the intermediate and can further react with $OH^{\bullet}$ to form HNO_3 (Eq. (5)). To evaluate the further conversion from NO_2 to HNO_3, the conversion rate of NO_2 was defined as follows:

$$NO_2 \ \text{conversion}\,(\%) = \frac{[NO]_{inlet} - [NO_x]_{outlet}}{[NO]_{inlet} - [NO]_{outlet}} \times 100\% \quad (6)$$

where $[NO]_{outlet}$ and $[NO_x]_{outlet}$ were the outlet concentrations measured at an irradiation time of 120 min after the UV lamp was turned on. The conversion rates of NO_2 are shown in Table 1. It can be seen that the NO_2 conversion rate is over 50% when calcination temperature is not higher than 300 °C. At 500 °C, however, it decreases significantly due to the less TiO_2 photocatalysts on the surface of the glass fibers. Therefore, to obtain the TiO_2-coated glass fibers with highly photocatalytic activity, the clacination temperature should be kept at or below 300 °C.

Table 1
Effects of calcination temperatures on the photocatalytic activity of the TiO_2 particles deposited on the glass fibers

Temperature (°C)	NO removal (%)	NO_2 removal (%)	NO_x removal (%)	NO_2 conversion (%)
60	55.5	−24.9	30.6	55.2
300	64.9	−29.6	35.2	54.3
500	19.4	−17.8	1.6	8.2

3.3. Effect of irradiation time and reaction cycles on the photocatalytic activity

It is important for a photocatalyst to have a long-term and repeated photocatalytic activity, which can reduce the times of photocatalyst replacement. Fig. 4 shows the effect of irradiation time on photocatalytic activity of the TiO_2 particles deposited on the glass fibers at 60 °C for the photocatalytic oxidation of 200 ppb NO. It can be seen that the concentration of NO slightly increases with increasing UV irradiation time. This indicates that the TiO_2 particles deposited on the glass fibers had a low deactivation rate even for 12 h UV irradiation. However, no deactivation was found in our previous study for the photocatalytic degradation of BETX (benzene, toluene, ethybenzene and *o*-xylene) [3]. The difference in the deactivation rate may be attributed to different pollutant concentrations and the amount of

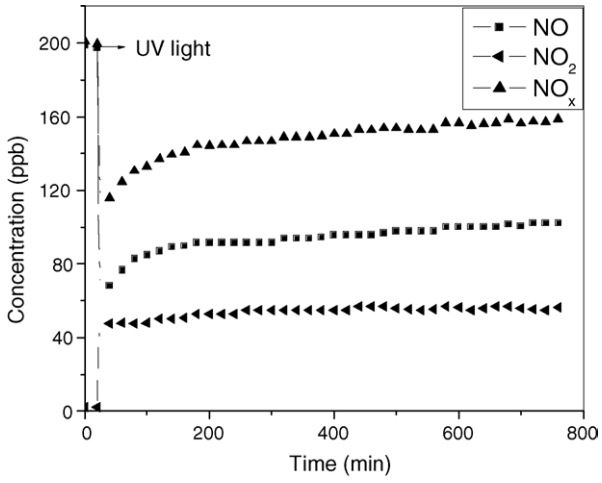

Fig. 4. Effect of irradiation time on photocatalytic activity of the TiO_2 particles deposited on the glass fibers at 60 °C for the photocatalytic oxidation of 200 ppb NO. Residence time: 11.4 min; humidity level: 2100 ppmv.

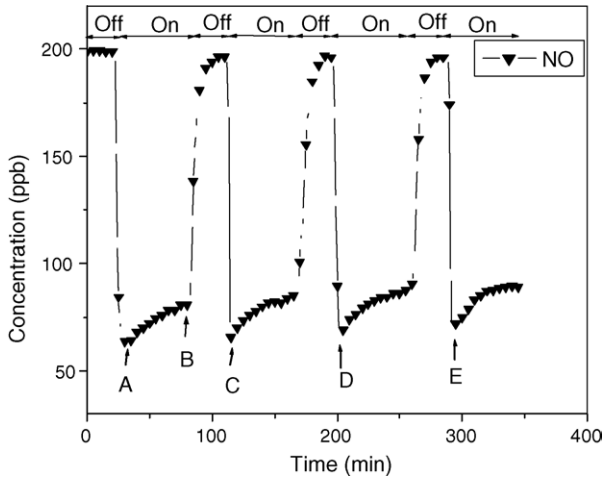

Fig. 5. Effect of reaction cycles on photocatalytic activity of the TiO_2 particles deposited on the glass fibers at 60 °C for the photocatalytic oxidation of 200 ppb NO. Residence time: 11.4 min; humidity level: 2100 ppmv.

the TiO_2 photocatalysts used. In our previous study, the BETX concentration was kept at ca. 35 ppb and the weight of the TiO_2 photocatalyst used was ca. 1.64 g. However, in this study, the NO concentration was maintained at ca. 200 ppb and the weight of the TiO_2 photocatalyst employed was lower than 0.5 g calculated according to the experimental conditions. Our previous results suggested that a higher pollutant concentration and less amount of TiO_2 photocatalyst might cause an obvious deactivation, while the deactivation was hardly observed when the concentration pollutants was very low and more photocatalyst was applied in a reaction system [2,3]. Other researchers also reported a similar deactivation of catalyst when pollutant concentrations were high (several hundreds ppm) [30,31].

Fig. 5 shows the effect of reaction cycles on photocatalytic activity of the TiO_2 particles deposited on the glass fibers at 60 °C for the photocatalytic oxidation of 200 ppb NO. After adsorption and desorption reached equilibrium, the UV light was turned on for 1 h and then turned off for 30 min to recover to the equilibrium status of adsorption and desorption. This process was repeated for four times to evaluate the effect of reaction cycles on the photocatalytic activity of the TiO_2-coated glass fibers. It was found that when the UV lamp was turned on, NO concentration decreased rapidly and reached a lowest value. Then, with increasing UV irradiation time, the NO concentration gradually increased from 66.0 ppb (A) to 81.3 ppb (B). This could be ascribed to the decreasing number of the active sites of TiO_2 particles due to the formation of HNO_3. However, it should be noted that at the following reaction cycle, a similar low NO concentration of 66.5 ppb (C) could also be obtained at the beginning of UV irradiation and then the photocatalytic oxidation of NO showed a similar process to the former photogradation reaction (from A to B). It could be inferred that the previous reaction cycles had no an obvious effect on the photocatalytic activity of the TiO_2 particle samples. This phenomenon was also observed in the further repeated photocatalytic oxidation experiments of NO, as shown in the Fig. 5 (D and E). When UV lamp was turned on, the NO molecules were photocatalytically oxidized into NO_2 and then further oxidized into HNO_3. The formed HNO_3 would be probably adsorbed to the active sites of TiO_2 photocatalyst and led to the decrease of photocatalytic activity of TiO_2 particles. In this study, however, it was found that the photocatalytic activity of the TiO_2 particles deposited on the glass fibers was not obviously affected by the previous photocatalytic reactions. Therefore, it was reasonable to suggest that the HNO_3 adsorbed on the active sites could transfer to non-active sites of TiO_2 particles or the surface of the glass fibers and then recovered to a surface similar to the virgin TiO_2 before UV irradiation. Another possible reason was that the NO_2 intermediate might accumulate on the active sites of TiO_2 particles and let the TiO_2 photocatalyst deactivate. When UV lamp was turn off, the NO_2 molecules could transfer into the air steam due to the competitive adsorption of NO molecules, leading to the recovery of active sites on the surface of TiO_2 particle photocatalyst.

3.4. Comparison of photocatalytic activity of TiO_2 particles and thin films

To further evaluate the photocatalytic activity and the deactivation rate of the TiO_2 particles deposited on the glass fibers, the TiO_2 film was also prepared on the stainless steel substrate under the same deposition conditions. Fig. 6 shows a typical surface morphology of the as-prepared TiO_2 film deposited on the stainless steel and dried at 60 °C. The TiO_2 film is composed of many TiO_2 particles with a size of 50–100 nm. Further, observation indicates that the TiO_2 particles are the aggregates of many smaller TiO_2 particles with a size of 20–50 nm, which was similar to the image of the TiO_2 particles deposited on the glass fibers (as shown in Fig. 1). Fig. 7 shows the comparison of photocatalytic activity of the TiO_2 particles deposited on the glass fiber and TiO_2 thin film on the stainless steel for the photocatalytic oxidation of 200 ppb NO. Compared with the TiO_2 particles deposited on the glass fibers, the TiO_2 film shows a higher photocatalytic activity at the beginning of photocatalytic reaction. However, the photocatalytic activity of TiO_2 film decreases rapidly. After 70 min, the photocatalytic activity of the TiO_2 particles deposited on the glass fiber is higher than that of

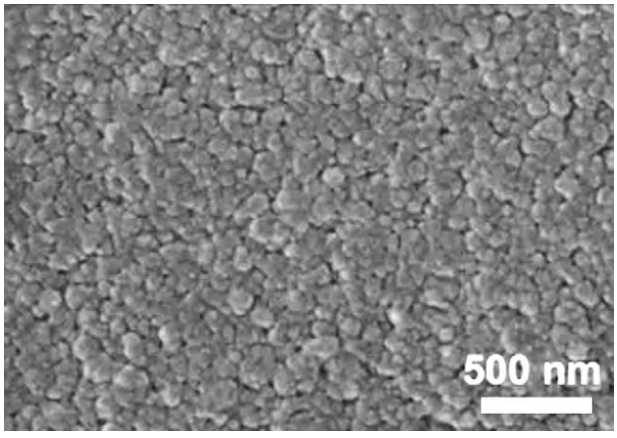

Fig. 6. SEM image of the TiO_2 film deposited on the stainless steel at 60 °C.

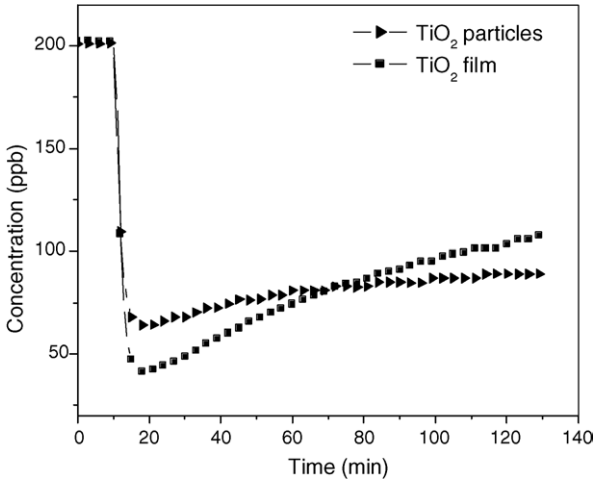

Fig. 7. Comparison of photocatalylic activity of the TiO_2 particles deposited on the glass fiber and TiO_2 thin films on stainless steel for the photocatalytic oxidation of 200 ppb NO. Deposition temperature: 60 °C; residence time: 11.4 min; humidity level: 2100 ppmv.

TiO_2 thin film on the stainless steel, indicating that the TiO_2 particles deposited on the glass fiber exhibits a lower deactivation rate for the photocatalytic oxidation of NO. This further confirms that the formed HNO_3 from the photocatalytic oxidation of NO can diffuse to the surface of glass fibers due to its larger surface area. On the contrary, for the TiO_2 film deposited on the stainless steel, the photocatalytic reaction of NO occurs on the surface of the film and no other space can be used for the diffusion and transfer of HNO_3. Therefore, the accumulation of HNO_3 on the surface of the TiO_2 film leads to a higher deactivation rate.

4. Conclusion

Anatase TiO_2 particles could be uniformly and dispersedly deposited on the surface of the glass fibers by a LPD method using TiF_4 as the precursor at 60 °C. Calcination temperature obviously influenced the surface morphology and photocatalytic activity of the TiO_2 particles deposited on the glass fibers. When the calcination temperature was not higher than 300 °C, the TiO_2 samples showed a high photocatalytic activity for the photocatalytic oxidation of NO and for the further conversion of NO_2 (from NO_2 to HNO_3). In contrast, at 500 °C, the sample exhibited a low photocatalytic activity due to the dropping of TiO_2 particles from the glass fibers. Compared with the TiO_2 film photocatalyst, the TiO_2 particle photocatalyst prepared by this method could maintain a long-term and repeated photocatalytic activity and a low deactivation rate.

Acknowledgements

This work was partially supported by the National Natural Science Foundation of China (50272049, 20473059). This work was also financially supported by the Excellent Young Teachers Program of MOE of China, Project-Sponsored by SRF for ROCS of SEM of China and the Dean Reserve Fund from the Hong Kong Polytechnic University.

References

[1] A.P. Jones, Atoms. Environ. 33 (1999) 4535.
[2] C.H. Ao, S.C. Lee, Appl. Catal. B44 (2003) 191.
[3] C.H. Ao, S.C. Lee, C.L. Mak, L.Y. Chan, Appl. Catal. B 42 (2003) 119.
[4] S.O. Baek, Y.S. Kim, R. Perry, Atoms. Environ. 31 (1997) 529.
[5] S.C. Lee, N.H. Kwok, H. Guo, W.T. Hung, Sci. Total Environ. 302 (2003) 75.
[6] S.C. Lee, L.Y. Chan, Environ. Int. 24 (1998) 729.
[7] C.J. Weschler, H.C. Shields, D.V. Naik, Environ. Sci. Technol. 28 (1994) 2120.
[8] C.H. Ao, S.C. Lee, J.C. Yu, J. Photochem. Photobiol. A156 (2003) 171.
[9] F.I. Khan, A.K. Ghoshal, J. Loss Prev. Process Ind. 13 (2000) 527.
[10] K. Honda, A. Fujishima, Nature 238 (1972) 37.
[11] H. Tada, M. Yamamoto, S. Ito, Langmuir 15 (1999) 3699.
[12] J.G. Yu, M.H. Zhou, B. Cheng, H.G. Yu, X.J. Zhao, J. Mol. Catal. A 227 (2005) 75.
[13] J.G. Yu, H.G. Yu, B. Cheng, X.J. Zhao, J.C. Yu, W.K. Ho, J. Phys. Chem. B 107 (2003) 13871.
[14] F.B. Li, X.Z. Li, Appl. Cata. A228 (2002) 15.
[15] J. Peral, D.F. Ollis, J. Catal. 136 (1992) 554.
[16] J.G. Yu, J.C. Yu, M.K.P. Leung, W.K. Ho, B. Cheng, X.J. Zhao, J.C. Zhao, J. Catal. 217 (2003) 69.
[17] J.C. Yu, W.K. Ho, J. Lin, H. Yip, P.K. Wong, Environ. Sci. Technol. 37 (2003) 2296.
[18] X.Z. Li, F.B. Li, Environ. Sci. Technol. 35 (2001) 2381.
[19] J.C. Yu, J.G. Yu, W.K. Ho, Z.T. Jiang, L.Z. Zhang, Chem. Mater. 14 (2002) 3808.
[20] H. Kishimoto, K. Takahama, N. Hashimoto, Y. Aoi, S. Deki, J. Mater. Chem. 8 (1998) 2019.
[21] G. Balasubramanian, D.D. Dionysiou, M.T. Suidan, Y. Subramanian, I. Baudin, J.M. Laine, J. Mater. Sci. 38 (2003) 823.
[22] H. Nagayama, H. Honda, H. Kawahara, J. Electrochem. Soc. 135 (1988) 2013.
[23] H. Pizem, C.N. Sukenik, U. Sampathkumaran, A.K. McIlwain, M.R. De Guire, Chem. Mater. 14 (2002) 2476.
[24] Y. Masuda, S. Ieda, K. Koumoto, Langmuir 19 (2003) 4415.
[25] S. Deki, Y. Aoi, O. Hiroi, A. Kajinami, Chem. Lett. 6 (1996) 433.
[26] H.G. Yu, S.C. Lee, C.H. Ao, J.G. Yu, J. Cryst. Growth 280 (2005) 612.
[27] I. Ibusuki, K. Yakeuchi, J. Mol. Catal. 88 (1994) 93.
[28] Y. Komazaki, H. Shimizu, S. Tanaka, Atoms. Environ. 33 (1999) 4363.
[29] S. Matsuda, H. Hatano, A. Tsutsumi, Chem. Eng. J. 82 (2001) 183.
[30] O. Hennezel, D.F. Ollis, J. Catal. 167 (1997) 118.
[31] R.M. Alberici, W.F. Jardim, Appl. Catal. B 14 (1997) 55.